International Journal of Pressure Vessels and Piping 88 (2011) 198–212

Contents lists available at ScienceDirect

International Journal of Pressure Vessels and Piping

journal homepage: www.elsevier.com/locate/ijpvp

Design of pressure vessels using shape optimization: An integrated approach

R.C. Carbonari [a], P.A. Muñoz-Rojas [b], E.Q. Andrade [c], G.H. Paulino [d,e], K. Nishimoto [f], E.C.N. Silva [a,*]

[a] Department of Mechatronic Engineering, Escola Politécnica da Universidade de São Paulo, Av. Prof. Mello Moraes, 2231 São Paulo, SP 05508-900, Brazil
[b] Department of Mechanical Engineering, Universidade do Estado de Santa Catarina, Bom Retiro, Joinville, SC 89223-100, Brazil
[c] CENPES, PDP/Métodos Científicos, Petrobras, Brazil
[d] Newmark Laboratory, Department of Civil and Environmental Engineering, University of Illinois at Urbana-Champaign, 205 North Mathews Av., Urbana, IL 61801, USA
[e] Department of Mechanical Science and Engineering, University of Illinois at Urbana-Champaign, 158 Mechanical Engineering Building, 1206 West Green Street, Urbana, IL 61801-2906, USA
[f] Department of Naval Architecture and Ocean Engineering, Escola Politécnica da Universidade de São Paulo, Av. Prof. Mello Moraes, 2231 São Paulo, SP 05508-900, Brazil

ARTICLE INFO

Article history:
Received 7 September 2010
Received in revised form
10 May 2011
Accepted 11 May 2011

Keywords:
Shape optimization
Pressure vessel
Multi-objective function

ABSTRACT

Previous papers related to the optimization of pressure vessels have considered the optimization of the nozzle independently from the dished end. This approach generates problems such as thickness variation from nozzle to dished end (coupling cylindrical region) and, as a consequence, it reduces the optimality of the final result which may also be influenced by the boundary conditions. Thus, this work discusses shape optimization of axisymmetric pressure vessels considering an integrated approach in which the entire pressure vessel model is used in conjunction with a multi-objective function that aims to minimize the von-Mises mechanical stress from nozzle to head. Representative examples are examined and solutions obtained for the entire vessel considering temperature and pressure loading. It is noteworthy that different shapes from the usual ones are obtained. Even though such different shapes may not be profitable considering present manufacturing processes, they may be competitive for future manufacturing technologies, and contribute to a better understanding of the actual influence of shape in the behavior of pressure vessels.

1. Introduction

In the pressure vessel literature, the optimization of nozzle and heads has been conducted independently. Although this is a practical and widely used approach, it leads to undesirable problems such as thickness variation from nozzle to head (among others) and, as a consequence, reduces the optimality of the final result (which may also be influenced by the adopted boundary conditions). Thus, this work investigates the optimization of pressure vessels considering a model of the entire vessel. A multi-objective function based on a p-root of summation of p-exponent terms of von-Mises stress values is defined in order to minimize the tank maximum von-Mises stresses. Mechanical and thermal loads are considered. Shape optimization techniques are applied, and the design optimization procedure is implemented by combining the commercial finite element analysis system ANSYS with our MATLAB optimization algorithm. Although composite tanks have a strength/weight ratio higher than steel tanks, they have a higher manufacturing cost. Thus, this work emphasizes homogeneous tanks, and focuses on CNG (Compressed Natural Gas) tank design by means of shape optimization techniques.

This paper is organized as follows. The literature review and related work are presented in Section 2. The formulation and numerical implementation of the optimization problem for the pressure vessel is described in Sections 3 and 4, respectively. In Section 5, the optimized shapes for the entire pressure vessel are presented and the results are discussed. Finally, in Section 6, some conclusions are inferred.

2. Related work

The design of pressure vessels is an important and practical topic which has been explored for decades. Even though optimization techniques have been extensively applied to design structures in general, few pieces of work can be found which are directly related to optimal pressure vessel design. These few references are mainly related to the design optimization of homogeneous and composite pressure vessels.

A pioneering work on optimization techniques for designing pressure vessels was presented by Middletown and Owen [1], who

* Corresponding author. Tel.: +55 11 30919754; fax: +55 11 30915722.
E-mail addresses: ronny@usp.br (R.C. Carbonari), pablo@joinville.udesc.br (P.A. Muñoz-Rojas), edmundoq@petrobras.com.br (E.Q. Andrade), paulino@uiuc.edu (G.H. Paulino), knishimo@usp.br (K. Nishimoto), ecnsilva@usp.br (E.C.N. Silva).

0308-0161/$ – see front matter © 2011 Elsevier Ltd. All rights reserved.
doi:10.1016/j.ijpvp.2011.05.005

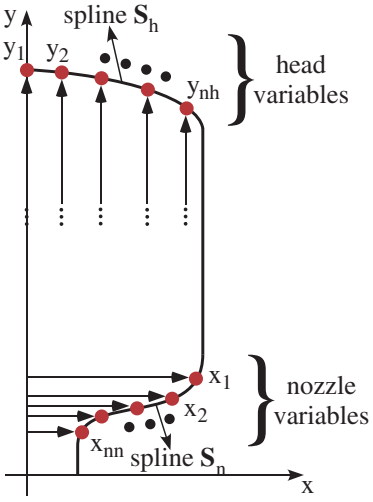

Fig. 1. Definition of design variables.

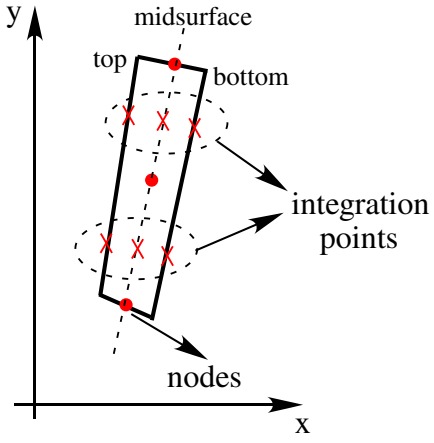

Fig. 3. Details of the shell element (employed in this work).

used parametric optimization techniques to minimize the maximum shear stress in the design of a pressure vessel dished end (head) modeled with axisymmetric finite elements. Following this work, Middletown [2] applied these parametric optimization techniques to design a pressure vessel nozzle considering the minimization of the maximum shear stress. Mechanical and thermal loads were taken into account by specifying different temperatures in the internal and external walls of the nozzle and dished end (head). Later, Blachut [3] also applied parametric optimization techniques to minimize the weight of the dished end by considering the limit pressure instead of mechanical stress. The limit pressure was defined as the value that first causes a full plastic region along the entire thickness of the pressure vessel. The optimization problem was defined as the minimization with constraints of the limit pressure, the strain at the peak of the dished end, and box constraints for parametric design variables. A zero order method (no gradients) was applied to solve the optimization problem. Four situations were studied: optimization of the main dimensions of a torispherical shell; optimization of the elliptical profile of the torispherical shell with uniform thickness; the same problem, but including the thickness as a design variable; and again the same problem, however, considering the thickness varying along the meridian defined by a polynomial. The weight reduction obtained was 8%, 19%, 27%, and 31%, respectively. As an important conclusion, they showed that *the boundary conditions between the dished end and the cylinder do influence the design*. A "Fully Stressed Design"-(FSD), which keeps the stress constant along the body, was also performed, however, it produced inferior results in relation to the best result among the four cases discussed, showing that, as expected, the design considering stress constraints is not as intuitive and thus a more formal approach is needed.

Another relevant work considering pressure vessel design using computational modeling was presented by Zhu and Boyle [4], who applied shape optimization techniques to optimize separately the head and nozzle of the pressure vessel, considering as objective function either the mechanical stresses or the limit pressure. The limit pressure is calculated by using the elastic compensation method [5–7], and performing successive linear analyses, which has as main advantage the fact that it precludes the need to

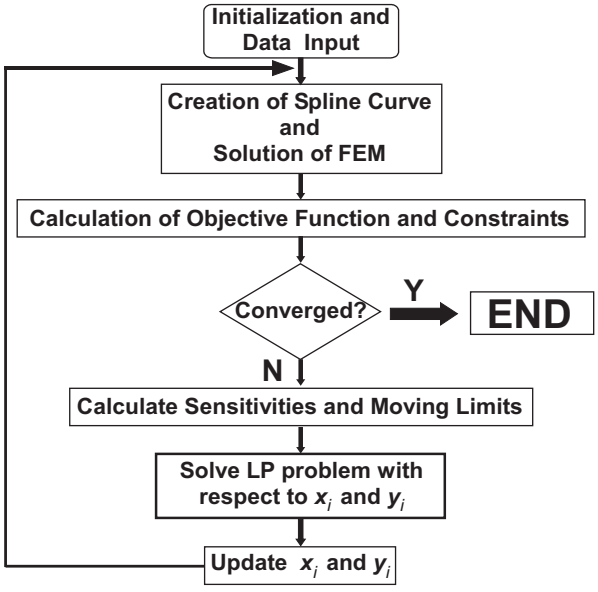

Fig. 2. Flowchart of optimization procedure.

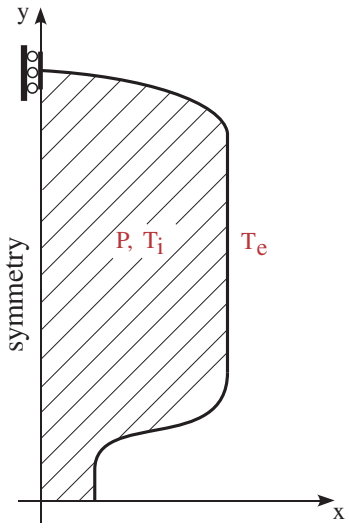

Fig. 4. Computer-aided Engineering (CAE) model including pressure (P), temperature (T_i, T_e), and boundary conditions.

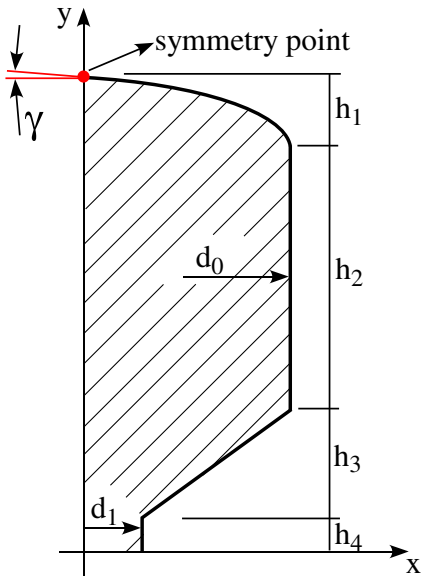

Fig. 5. Initial pressure vessel shape.

perform non-linear analysis, thus reducing the computational cost in the overall optimization procedure. Their optimization procedure was implemented using the software ANSYS with the APDL (ANSYS Parametric Design Language) language and spline curves to perform shape optimization. The obtained results showed satisfactory improvements. The work of Malinowski and Magnuki [8] employed parametric discrete optimization techniques to design internal reinforcements of pressure vessels by minimizing the reinforcement mass considering stress constraints. Following an analytical approach, Banichuk et al. [9] used variational calculus to find the head meridian profile optimal curve in order to maximize the ratio between head volume and mass subjected to stress constraints.

An interesting issue when designing the head (or nozzle) is the stress concentration in the transition between the head (or nozzle) and the cylinder. At the head and cylinder junction, bending moments and shear forces appear in order to compensate the stiffness difference between the components (head and cylinder). These bending moments and shear forces generate a stress concentration that can be estimated by thin shell theory. When a non-hemispherical head is considered, the stress concentration along the junction increases. Such stress concentration can be reduced either by transitioning the thickness from the head to the cylinder or by changing the head geometry. Following this idea, Magnucki and Lewinsky [10] analytically assessed the head geometry (shape) design that generates an equivalent stress less than or equal to the cylinder stress. In this case, the internal bending moments and shear forces would be null. They considered a head geometry partially composed by a sphere and a generic curve (to be determined). The sphere radius is calculated to generate equivalent stresses in the head that do not exceed the equivalent stress at the cylinder surface. The stress is uniform and the thickness is uniform for the proposed geometry. An equivalent ellipsoidal head would have an equivalent stress value in the head 20% larger than the equivalent stress in the cylinder and a head thickness 50% larger than the cylinder thickness. The minimization of stress concentration in pressure vessels with ellipsoidal heads was also discussed by Magnucki et al. [11] by means of analytical techniques. As noticed in their previous work, if the same thickness is considered for head and cylinder, there is a stress concentration in the junction of head and cylinder with head stresses being larger than cylinder stresses. A stress equalization can be obtained by increasing the head thickness or by changing the head geometry $b/a > 0.5$, where b and a are the minor and major ellipse axes, respectively. In the case of thickness variation, an increase of 70% from cylinder to head would be necessary, which is impractical from a manufacturing point of view. An interesting plot of thickness ratio as a function of (b/a) ratio related to the non-dimensional equivalent stress equalization between head and cylinder could be built. From this plot, by considering the same thickness for head and cylinder, the ratio (b/a) must be equal to 0.6 for stress equalization. In another plot, the ratio between the maximum non-dimensional equivalent stress and the cylinder equivalent stress (subjected to pressure only) is given as a function of the ratio (b/a). It shows that (b/a) values less than 0.48 are not of interest because the stress concentration would increase. For (b/a) values ranging from 0.48 to 0.86, high stress values are generated (although equal for head and cylinder). Thus, other criteria, such as minimum mass, must be selected to decide on a (b/a) value between 0.48 and 0.86. From these previous pieces of work, we conclude that heads with hemispherical, torispherical or elliptical geometries are not optimal because they can only avoid the stress concentration in the junction between head and cylinder with large thickness variation, which may be impractical (e.g. from a manufacturing point of view). Meanwhile, it is also concluded that the minimization of the stress concentration in the junction can be achieved by changing the head meridian profile shape, suggesting that shape optimization techniques can be applied to search for this optimum shape. The same study could be developed for the junction between nozzle and cylinder, however, no analytical work has been found, probably, due to difficulties to develop the analytical model. However, similar conclusions may be applied, that is, by changing the nozzle meridian profile shape the stress concentration in the transition can be reduced.

Table 2
Initial values for design variables (mm).

initial shape 1	initial shape 2	initial shape 3	elliptical head
y_1 (0; 3066)	y_1 (0; 3066)	y_1 (0; 3066)	y_1 (0; 2066)
y_2 (500; 2932)	y_2 (382.7; 2989.9)	y_2 (258.8; 3.31.9)	y_2 (223; 2053)
y_3 (866; 2566)	y_3 (707.1; 2773.1)	y_3 (500; 2932)	y_3 (434; 2016)
x_1 (900; 893)	y_4 (923.9; 2448.7)	y_4 (707.1; 2773.1)	y_4 (624; 1957)
x_2 (800; 719)	x_1 (900; 893)	y_5 (866; 2560)	y_5 (782; 1877)
x_3 (700; 546)	x_2 (800; 719)	y_6 (965.9,2324.8)	y_6 (901; 1783)
x_4 (600; 373)	x_3 (700; 546)	x_1 (900; 893)	y_7 (975; 1677)
	x_4 (600; 373)	x_2 (800; 719)	x_1 (900; 893)
		x_3 (700; 546)	x_2 (800; 719)
		x_4 (600; 373)	x_3 (700; 546)
			x_4 (600; 373)

Table 1
Material properties.

Young's Modulus	E	200.0×10^9	Pa
Poisson's Ratio	ν	0.3	
Density	ρ	7810.0	Kg/m^3
Thermal expansion	α	1.15×10^{-5}	1/°C

Table 3
Representative optimization parameters.

p	1 to 8
w	0.5
α_h	0.25
α_n	0.5
$\phi_h = \phi_n = 0.01$	

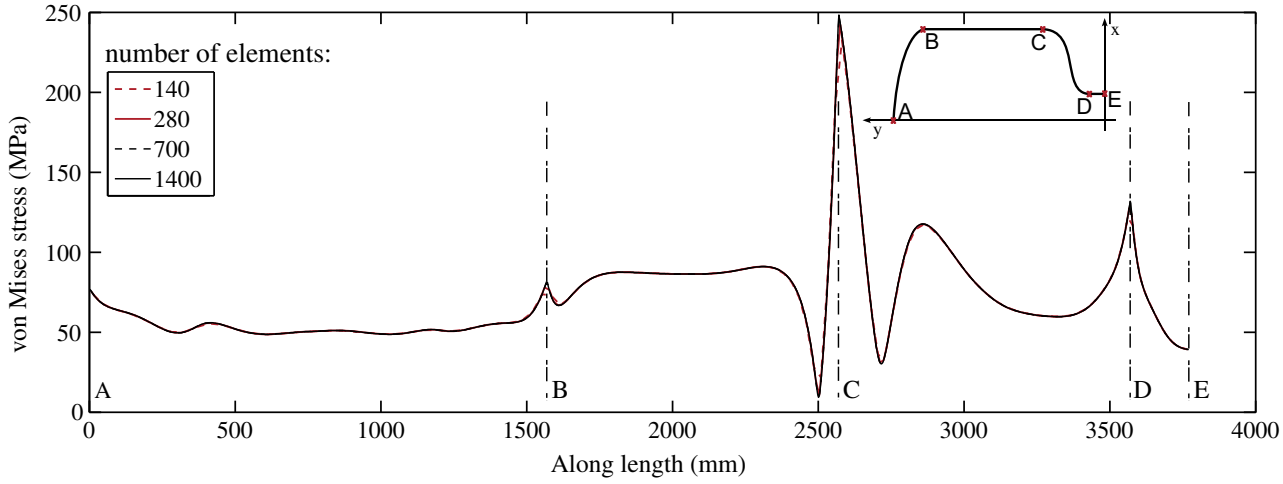

Fig. 6. von-Mises stress values along vessel meridional profile, considering different discretizations and no thermal load.

Although most of previous optimization literature assumed specific geometries, Hammer and Olhoff [12] used topology optimization to design structures subjected to pressure loads. For such design-dependent problem, the boundary where the pressure is applied must move as the material is removed. This problem is addressed by using a spline function to represent the boundary where the pressure is applied. A follow up of this work was provided by Du and Olhoff [13] and Zheng et al. [14], who extended the investigation to three-dimensional structures. However, they considered as objective function the minimization of mean compliance without stress constraints, which is not realistic for pressure vessel design. In fact, the solution of topology optimization considering stress constraints is still an open problem [15–17].

Recently, Blachut and Magnuki [18] published an extensive review about modeling and optimization of pressure vessels where they mention that, in the optimization field, there are still few pieces of work related to pressure vessel design. This work provides a contribution along those lines by presenting an integrated approach in which the entire vessel is considered in the optimization process.

3. Formulation of the shape optimization problem

In this section, an approach to design CNG tanks based on the shape optimization technique is presented. In this shape optimization approach, the head and nozzle meridian profile curves will be optimized by using spline curves, thus no predefined shape will be assumed. Shape here refers to the geometric shape of the midsurface with a uniform thickness. The shape of the midwall surface is more important than thickness for either maximum stress or load-carrying capacity [4]. A typical optimization problem is defined as

$$\begin{aligned} &\text{Min} && F(\mathbf{x}) \\ &\text{Subjected to} && g(\mathbf{x}) \le 0 \\ & && \mathbf{x}_L \le \mathbf{x} \le \mathbf{x}_U \end{aligned}$$

where $F(\mathbf{x})$ is the objective function, $\mathbf{x}$ are the design variables, $g(\mathbf{x})$ are inequality constraints, and $\mathbf{x}_L$ and $\mathbf{x}_U$ are box constraints. The pressure vessel optimized design can be achieved by direct enforcement of maximum stress as constraints or, alternatively, by defining a stress measure to be minimized as objective function. In this work, we deal with the stress minimization problem by defining a multi-objective function based on a p-root of summation of p-exponent terms of von-Mises stresses. These stresses are the usual choice of stress measurement for pressure vessel design in the literature [10,11]. The von-Mises stresses are chosen instead of limit pressure [5–7] because the intention is to design the vessel for actual working conditions [4]. If different levels of mechanical stresses occur in nozzle and head regions in this work, then an

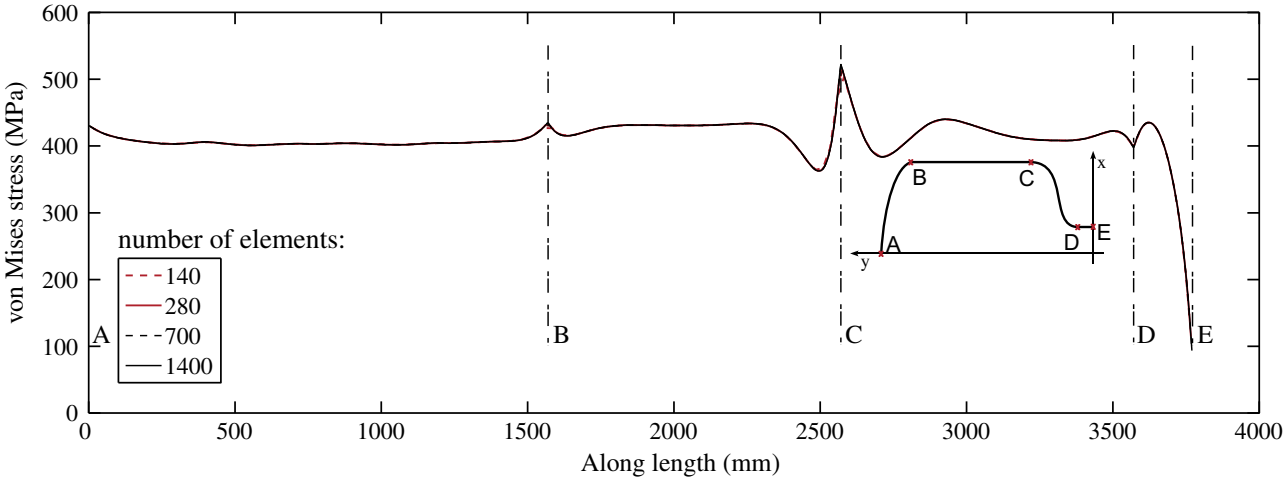

Fig. 7. von-Mises stress values along vessel meridional profile, considering different discretizations and thermal load.

analysis of the entire vessel is performed. A proper mathematical setting must be formulated in the sense that the optimization process should guarantee that nozzle and head stress values will have equal influence in the objective function. This is achieved by using a logarithmic function. Thus, a multi-objective function is defined as the sum of the logarithmic of the p-root of summation of p-exponent terms of head and nozzle von-Mises stresses, allowing the control of the head and nozzle stresses through a weighting coefficient, which it is given by:

$$F = w\ln\left(\sum_{i=1}^{nh}\sigma_{h_j}^{p}\right)^{\frac{1}{p}}+(1-w)\ln\left(\sum_{j=1}^{nn}\sigma_{n_j}^{p}\right)^{\frac{1}{p}} \quad (1)$$

where σ_{h_i} and σ_{n_j} are the von-Mises mechanical stresses at Gauss points of the $i-th$ and $j-th$ finite elements that model the head and nozzle, respectively; w is the weighting coefficient which allows control of the influence of stresses in the head and nozzle regions in the optimization problem; p is an exponent coefficient which can assume even or odd values (as von-Mises stress values are always positive); nh and nn are the number of finite elements used to discretize the head and nozzle regions, respectively. Therefore, the minimization of the multi-objective function consists of minimizing simultaneously the von-Mises mechanical stresses in the head and nozzle regions.

3.1. Design variables

In the adopted shape optimization approach the shapes of head and nozzle are given by cubic spline interpolation whose shape is changed during the optimization process by varying the coordinates of spline knots. Separate spline curves are defined for the head and for the nozzle. The optimization must be performed in a way that the spline knots move in the normal direction to the spline curve, because analytical shape sensitivity in the direction tangent to the spline can be shown to be null. In principle, $\boldsymbol{x}$ and $\boldsymbol{y}$ coordinates of spline knots could be chosen as design variables, however, considering the constraint that knots must move in the normal direction, it suffices to choose only $\boldsymbol{x}$ or $\boldsymbol{y}$ coordinates. Fig. 1 shows that $\boldsymbol{x}$ and $\boldsymbol{y}$ knot coordinates are chosen as the design variables for nozzle and head splines, respectively. Thus, the head design variable set is defined by the coordinates of the head spline knots ($\boldsymbol{y}_h$) in the Cartesian direction y, while the nozzle design variable set is defined by the coordinates of the nozzle spline knots ($\mathbf{x}_n$) in the Cartesian x direction, as illustrated in Fig. 1.

3.2. Complexity constraints

In order to reduce the numerical oscillations during the optimization process, and to control the spline shape, complexity

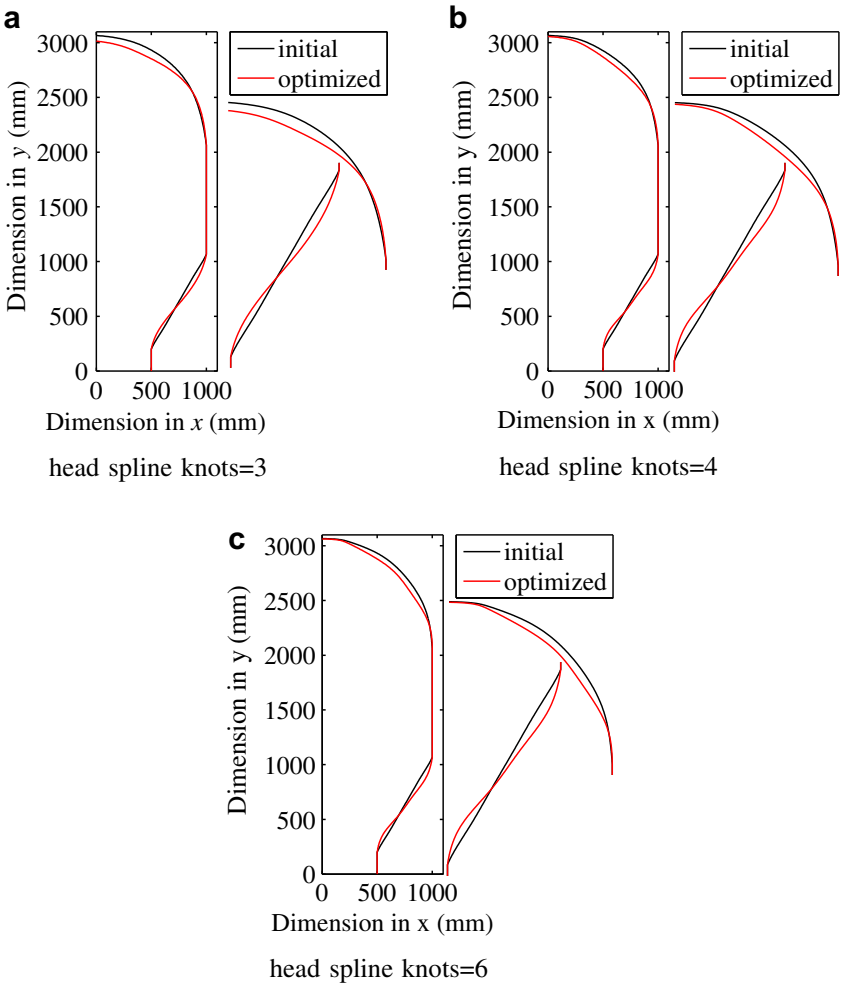

Fig. 8. Optimization result obtained for initial shapes 1, 2, and 3 corresponding to different number of head spline knots (no thermal load). Detailed views of head and nozzle are given beside each figure.

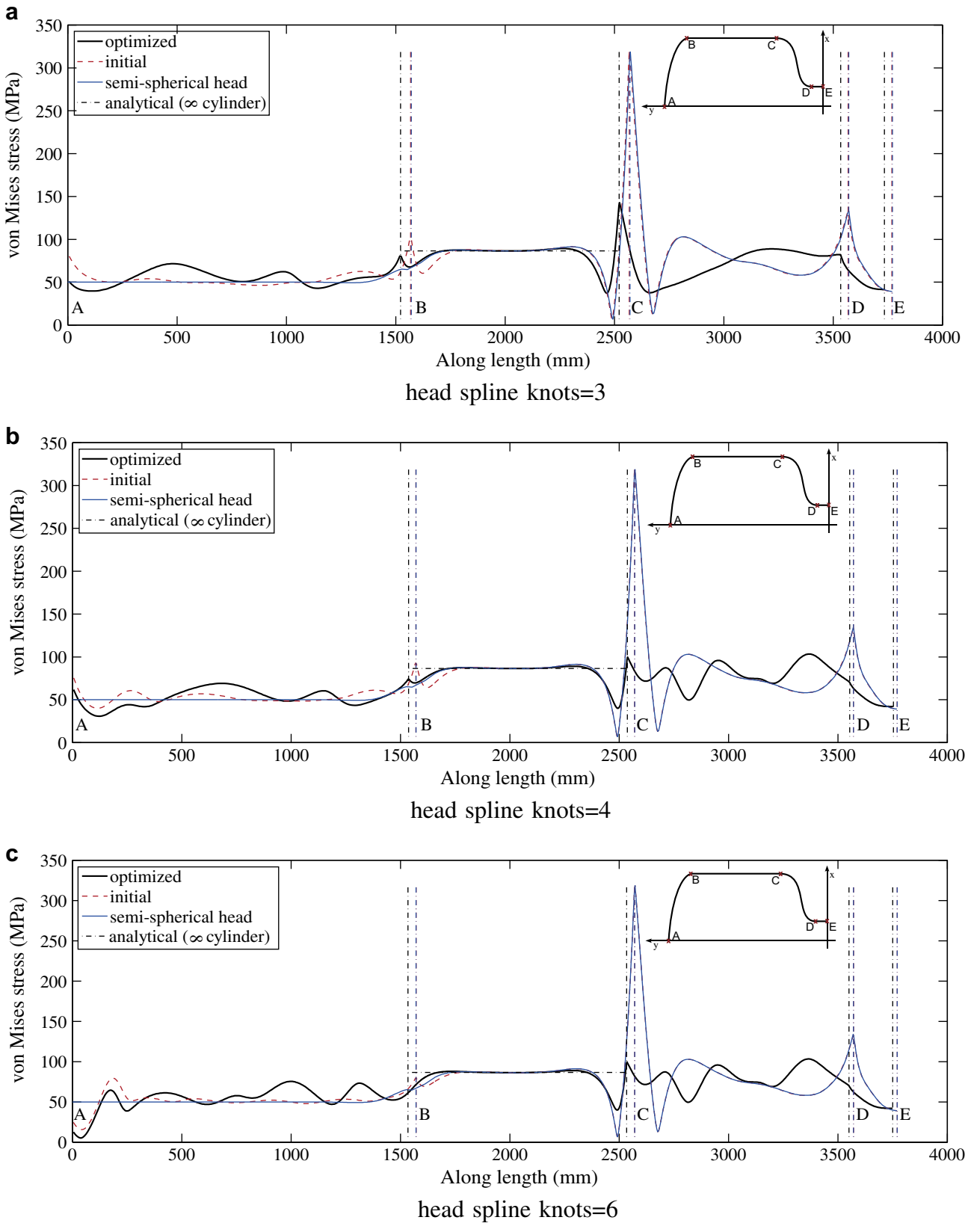

Fig. 9. von-Mises stress values along vessel optimized meridional profile for initial shapes 1, 2, and 3 corresponding to different number of head spline knots (no thermal load).

Table 4
Maximum von-Mises stress values (MPa), where subscripts $_h$, $_n$, $_0$, $_{ss}$, and h_2 indicate head, nozzle, initial shape, standard spherical, and cylindrical region h_2, respectively ($\sigma^a_{h_2} = 86.6$ Mpa for an infinite cylinder).

Example	σ_h	σ_{h0}	σ_{ss}	σ_n	σ_{n0}	σ_{h2}	σ_{h2_0}
Fig. 9(a)	80.4	101.3	67.0	142.9	318.6	89.0	91.5
Fig. 9(b)	73.9	92.9	67.0	103.3	318.6	89.0	91.5
Fig. 9(c)	75.6	79.4	67.0	103.4	318.6	89.0	91.5
Fig. 12(a)	303.5	292.0	261.6	276.6	452.7	276.5	278.0
Fig. 12(b)	302.1	286.5	261.6	276.6	452.7	276.5	278.0
Fig. 12(c)	256.6	276.2	261.6	276.6	452.7	276.5	278.0
Fig. 9(a, b and c)	thermal load						
Fig. 12(a, b and c)	no thermal load						

constraints are introduced in the optimization problem. Thus, the complexity constraints for the head region are defined as:

$$\begin{aligned} &y_1 \le y_{\max} \\ &y_1 - y_2 \ge \epsilon \\ &y_i - y_{i+1} \ge \epsilon \\ &y_{nh} \ge y_{\min} \quad (i = 2 \ldots nh-1) \end{aligned} \tag{2}$$

where y_i are shown in Fig. 1 and nh is the number of knots in the head region; $y_{\max}$ and $y_{\min}$ are the maximum and minimum values allowed for these coordinates, respectively; and ϵ is a small number. For the nozzle, the complexity constraints are defined as:

$$\begin{aligned} &x_1 \le x_{\max} \\ &x_1 - x_2 \ge \delta \\ &x_j - x_{j+1} \ge \delta \\ &x_{nn} \ge x_{\min} \quad (i = 2 \ldots nn-1) \end{aligned} \tag{3}$$

where x_i are shown in Fig. 1 and nn is the number of knots in the nozzle region; $x_{\max}$ and $x_{\min}$ are the maximum and minimum values allowed for these coordinates, respectively; and δ is a small number.

A material volume constraint is not specified because the change of spline length is not significant during the optimization. Although material volume constraint is not included, it is verified "a posteriori".

3.3. Summary and remarks

Based on the above considerations, shape optimization problem can be defined as:

$$\begin{aligned} &\text{Min}: \quad F(\mathbf{y}_h, \mathbf{x}_n) \\ &\text{Subjected to}: \\ &\quad y_1 \le y_{\max} \qquad x_1 \le x_{\max} \\ &\quad -y_1 + y_2 \le -\epsilon \quad -x_1 + x_2 \le -\delta \\ &\quad -y_i + y_{i+1} \le -\epsilon \quad -x_j + x_{j+1} \le -\delta \\ &\quad -y_{nh} \le -y_{\min} \quad (i = 2 \ldots nh-1) \\ &\quad -x_{nn} \le -x_{\min} \quad (j = 2 \ldots nn-1) \end{aligned}$$

The numerical implementation of this defined shape optimization problem is described in the next section. Mechanical (pressure) and thermal loads (temperature difference) are considered. In addition, in the case of vessels subjected to internal pressure, buckling instability may occur for head and nozzle (mainly head) if hoop stresses reach negative values [19]. The head buckling is more susceptible to occur for vessels with large diameter/thickness ratio and high yield stress values [20]. Because during the optimization process the head and nozzle geometry is changed, then a geometry susceptible to buckling problems may be obtained. In this work, no constraint is specified for the hoop stress in the optimization problem, its value is only verified "a posteriori" in the final result.

4. Numerical implementation of shape optimization program

The flowchart of the program is illustrated in Fig. 2. The program is implemented using the commercial software MATLAB [21] and ANSYS [22]. All processes, including the optimization process and file input and output from ANSYS are controlled by MATLAB. ANSYS input files contain all the information of the pressure vessel computer-aided engineering (CAE) model. After obtaining the input files, the MATLAB routine executes ANSYS, and an output file is generated, which is in turn read by MATLAB.

The pressure vessel is modeled by using the 2D-axisymmetric shell finite element type SHELL208 [22]. The default option for this element employs two nodes (linear displacement interpolation of the midsurface) and three integration points through the thickness (at the bottom, at the top and at the midsurface), as illustrated by Fig. 3. This element has the capability of modeling bending and membrane stiffness, and torsion. It gives, as a result, the longitudinal, meridional, and von-Mises stress values at the Gauss integration points. The von-Mises stress considered and presented for all results in this work are the maximum values among the Gauss integration points through the thickness.

Fig. 4 illustrates the mechanical and thermal boundary conditions applied to the model. In this figure, T_i and T_e are internal and external temperature, respectively, and P is the internal pressure.

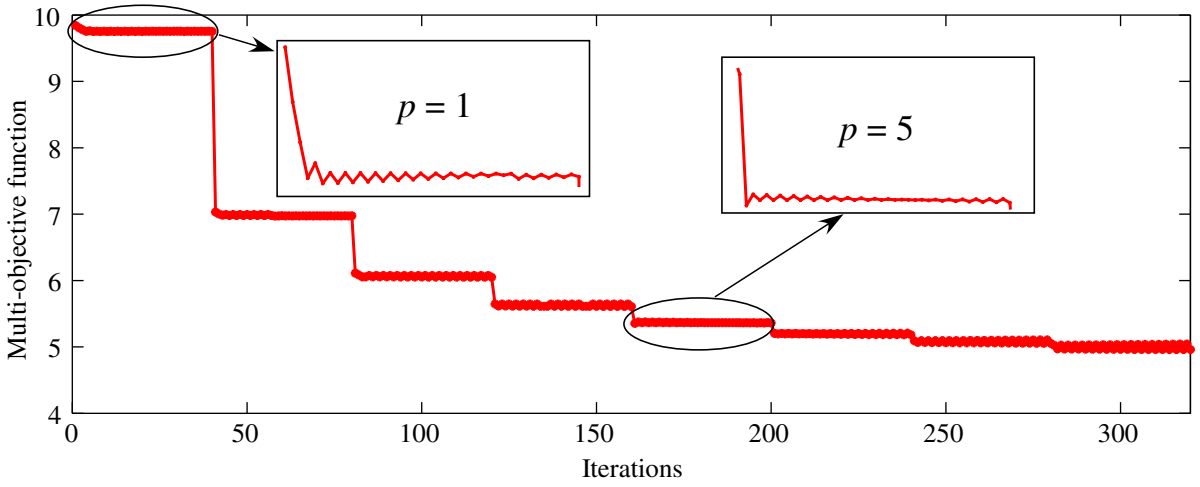

Fig. 10. Convergence of multi-objective function for initial shape 1, corresponding to head spline knot number equal to 3 (no thermal load).

Following the flowchart in Fig. 2, the initial data of the optimization problem is the geometry of the pressure vessel, which contains the spline knot coordinates (or design variable initial values), material properties, load and boundary conditions. The spline curves are obtained using the MATLAB function *spline*, considering the design variables y_h and x_n and discretization parameters *nh* and *nn* for head and nozzle, respectively. The used function *spline* considers a cubic spline data interpolation, which is generated using the following parameters:

$$\mathbf{S}_h = f(\mathbf{x}_h;\mathbf{y}_h) = [spline(h,x_i,1:nh);spline(h,y_i,1:nh)] \quad (4)$$

$$\mathbf{S}_n = f(\mathbf{x}_n;\mathbf{y}_n) = \left[spline(n,x_j,1:nn);spline\left(n,y_j,1:nn\right)\right] \quad (5)$$

where $\mathbf{S}_h$ and $\mathbf{S}_n$ are matrices that contain the cubic spline knot coordinates for the head and for the nozzle, respectively. The head spline $\mathbf{S}_h$ is obtained considering the tangent at the symmetry point equal to zero (see Fig. 5). As mentioned before, $\mathbf{x}_h$ and $\mathbf{y}_n$ are calculated as functions of $\mathbf{y}_h$ and $\mathbf{x}_n$, respectively, considering the constraint that knots must move in the normal direction.

In the sequence, the CAE model is defined including algorithmic parameters and mesh attributes such as the finite element type, number of nodes and elements, loads and boundary conditions. Once the CAE model is built, the ANSYS solver is executed by running a linear static analysis, which generates output files that contain the results of von-Mises mechanical stresses (σ_h and σ_n) at each finite element integration point.

The sensitivity analysis of the multi-objective function in relation to design variables is obtained by using the central finite difference scheme. Thus, for the gradient numerical calculations it is necessary to obtain the perturbations δ_h and δ_n defined in the expressions below,

$$\frac{\partial F}{\partial y_i} \cong \frac{F(y_i+\delta_h)-F(y_i-\delta_h)}{2\delta_h} \quad (6)$$

$$\frac{\partial F}{\partial y_i} \cong \frac{F(x_i+\delta_n)-F(x_i-\delta_n)}{2\delta_n} \quad (7)$$

Notice that *y* and *x* coordinates are defined as design variables for head and nozzle, respectively. Moreover, δ_h and δ_n are calculated considering a fraction of the spline length L_h or L_n, which is given by:

$$L_h = \frac{\oint_{j=1}^{nh} \mathbf{S}_h\left(x_j,y_j\right)ds}{\sum y_i} \Rightarrow \delta_h = \phi_h L_h \quad (8)$$

$$L_n = \frac{\oint_{i=1}^{nn} \mathbf{S}_n(x_i,y_i)ds}{\sum x_j} \Rightarrow \delta_n = \phi_n L_n \quad (9)$$

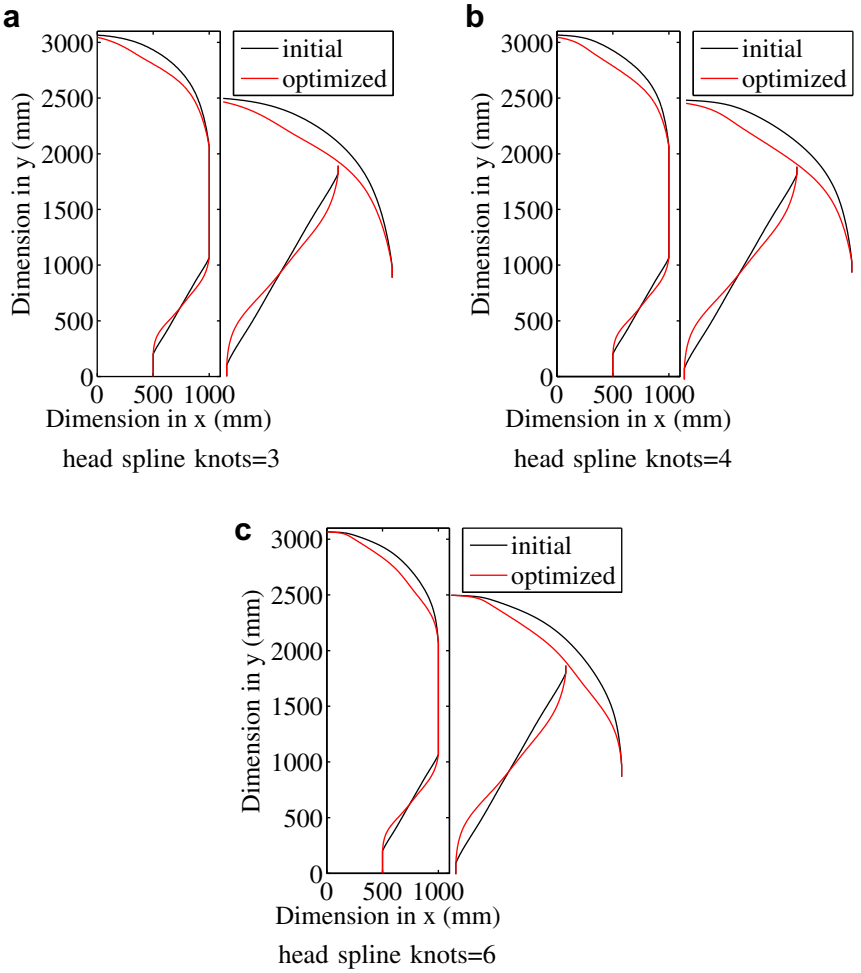

Fig. 11. Optimization result obtained for initial shapes 1, 2, and 3 corresponding to different number of head spline knot and with thermal load. Detailed views of head and nozzle are given beside each figure.

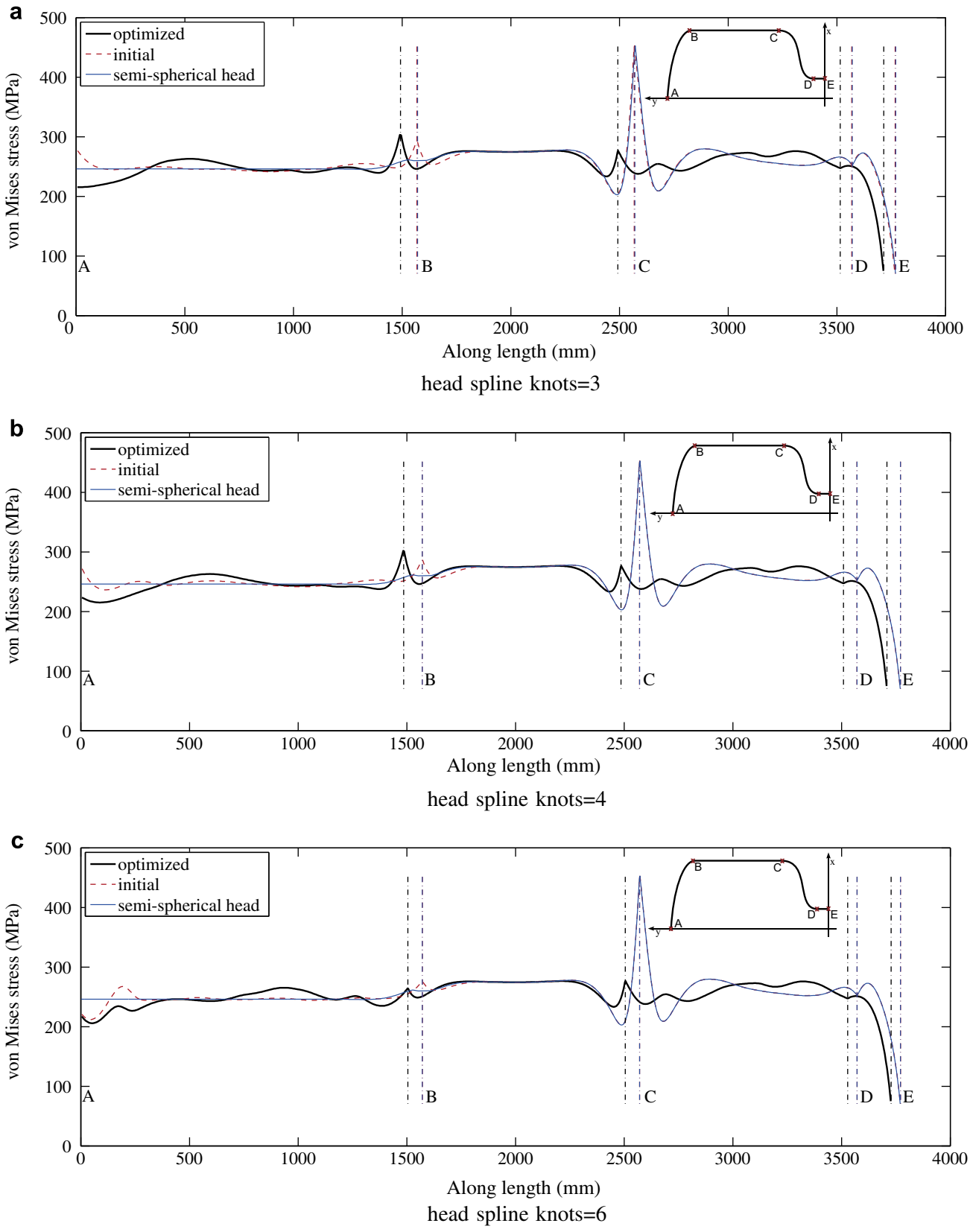

Fig. 12. von-Mises stress values along vessel optimized meridional profile for initial shapes 1, 2, and 3 corresponding to different number of knots at head spline and with thermal load.

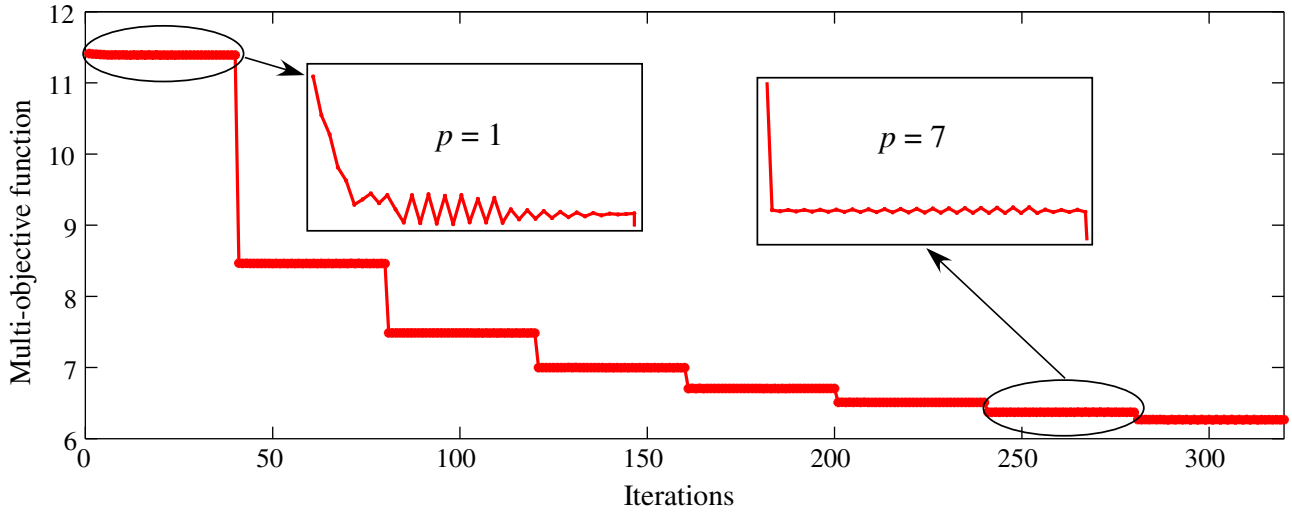

Fig. 13. Convergence of multi-objective function for initial shape 3, corresponding to head spline knot number equal to 6 and thermal load.

where ϕ_h and ϕ_n are percentage values specified for head and nozzle, respectively.

To solve the optimization problem, the gradient based sequential linear programming (SLP) optimization algorithm is used [23]. The SLP is implemented using the available function *linprog* (Linear Programming) from MATLAB. The SLP requires that a moving limit scheme be defined for design variables. These moving limits also help to control the numerical oscillations of multi-objective function gradients. The amplitude of the moving limits is defined as a function of coefficients θ_h and θ_n. These coefficients are calculated by using a scheme similar to the one used for calculating δ_h and δ_n. Thus, θ_h and θ_n are obtained considering a fraction of the spline length (L_h or L_n), which is given by:

$$\theta_h = \alpha_h L_h; \theta_n = \alpha_n L_n \tag{10}$$

where θ_h and θ_n are the moving limits coefficients for the head and nozzle, respectively, which are updated at each iteration. Accordingly, $\alpha_h$and α_n are percentage values specified for head and nozzle, respectively. Therefore, the upper and lower bounds obtained using the moving limits routine for the design variables are calculated by:

$$y_{i_L} = y_i - \theta_{hi}\lambda_i \tag{11}$$

$$y_{i_U} = y_i + \theta_{hi}\lambda_i \quad (i = 1 \ldots nh) \tag{12}$$

$$x_{j_L} = x_j - \theta_{nj}\lambda_j \tag{13}$$

$$x_{j_U} = x_j + \theta_{nj}\lambda_j \quad (j = 1 \ldots nn) \tag{14}$$

where subscripts $_L$ and $_U$ are lower and upper bounds, respectively. The parameters λ_i and λ_j are updated during the optimization process, and thus the moving limit steps decrease by 5% with the convergence of multi-objective function.

Thus, the following optimization problem at each iteration is defined:

$$\begin{aligned} &\text{Min :} && F(\mathbf{y}_h, \mathbf{x}_n) \\ &\text{Subjected to :} \\ &\quad y_1 \le y_{\max} && x_1 \le x_{\max} \\ &\quad -y_1 + y_2 \le -\epsilon && -x_1 + x_2 \le -\delta \\ &\quad -y_i + y_{i+1} \le -\epsilon && -x_j + x_{j+1} \le -\delta \\ &\quad -y_{nh} \le -y_{\min} && i = 2 \ldots nh \\ &\quad -x_{nn} \le -x_{\min} && j = 2 \ldots nn \\ &\quad y_{k_L} \le y_k \le y_{k_U} && k = 1 \ldots nh \\ &\quad x_{l_L} \le x_l \le x_{j_U} && l = 1 \ldots nn \end{aligned}$$

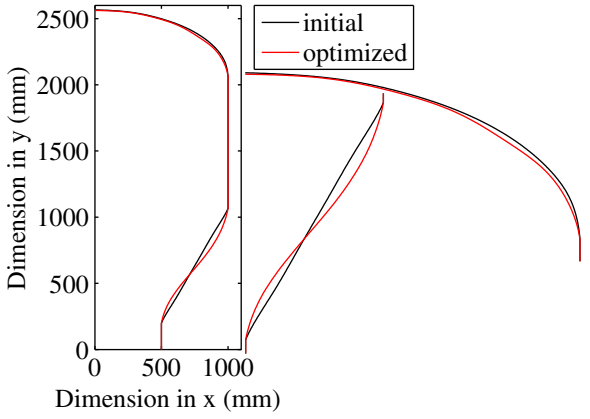

Fig. 14. Optimization result for example 2, considering $h_2 = 1000$ mm and free tangent angle at head symmetry knot (no thermal load). Detailed views of head and nozzle are given beside figure.

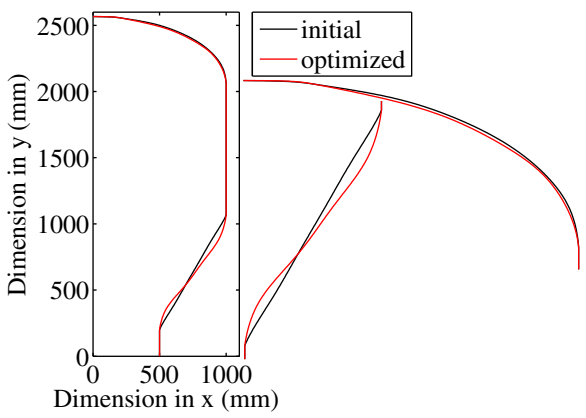

Fig. 15. Optimization result for example 2, considering $h_2 = 1000$ mm and null tangent angle at head symmetry point (no thermal load). Detailed views of head and nozzle are given beside figure.

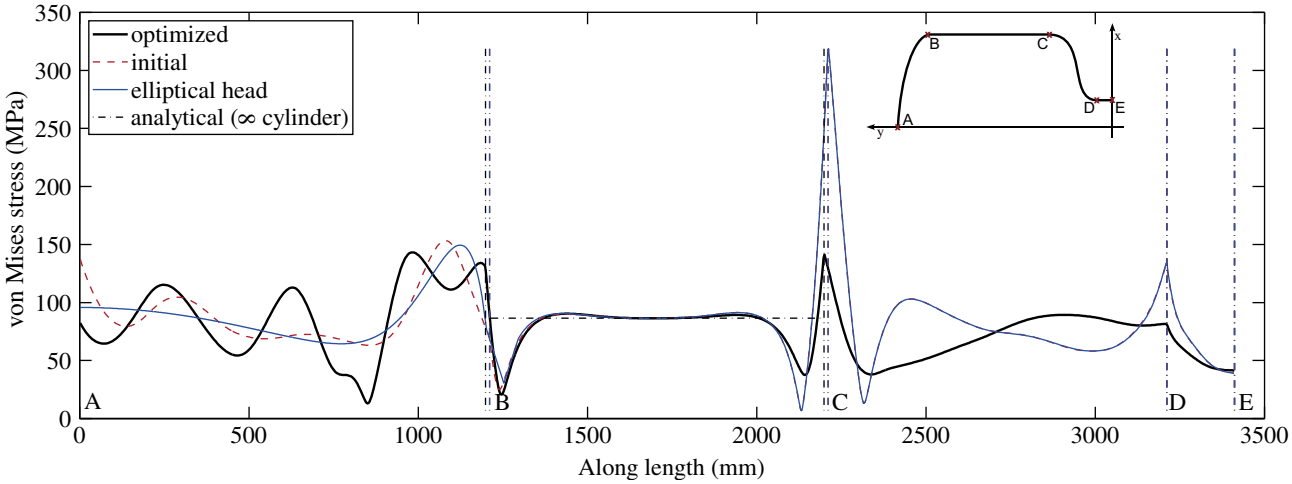

Fig. 16. von-Mises stress values along vessel optimized meridional profile obtained for example 2, considering $h_2 = 1000$ mm and free tangent angle at head symmetry point (no thermal load).

The optimization problem is updated with the new design variables and the loop is continued until convergence of the multi-objective function and, finally, the optimal shape of the vessel is obtained.

5. Numerical results

This section illustrates the integrated approach for pressure vessel design, in which the entire vessel is considered during the optimization process.

Fig. 5 shows the finite element model adopted for the vessel shape optimization. As indicated before, a 2D-axisymmetric shell element from ANSYS is used (SHELL 208). The material properties are described in Table 1. The initial vessel shape is depicted in Fig. 5, where the values of the parameters d_0, h_2, h_3, h_4, and d_1 are equal to 2000 mm, 1000 mm, 866 mm, 200 mm and 1000 mm, respectively. The corresponding initial values for the design variables that generate this geometry, considering spline approximations, are described in Table 2. These initial values for the vessel dimensions are based on reference [4]. The parameter h_1 depends on the initial design domain, and the influence of h_2 will be analyzed in Section 5.2.2. The thickness is uniform along the vessel profile and its value is equal to 10.0 mm. Examples are presented considering pressure load (P) equal to 1 MPa, and also pressure load together with thermal load. The thermal load is obtained by specifying a temperature gradient along the thickness. The p exponent value in Eq. (1) is changed continuously from 1 to 8, and the adopted parameter values for α_h and α_n (see Eq. (10)) are equal to 25% and 50%, respectively, for all examples. The coefficient w (see Eq. (1)) is equal to 0.5 for all examples. These parameters are summarized in Table 3.

5.1. Example 1: pressure vessel design with $\gamma = 0$

In this example, the objective is to analyze and compare the design of pressure vessels with mechanical loading only (pressure) and with both mechanical and temperature loading. An initial shape close (due to spline approximation) to a semi-sphere is adopted for the head ($h_1 = d_0/2$). The theoretical semi-spherical shape presents a uniform low value stress distribution, with a peak stress at the junction between cylinder and semi-sphere. Thus, it is a quasi-optimum result from the stress point of view, however, it is difficult to manufacture. Furthermore, it is a good initial guess to evaluate the optimization algorithm and its evaluation.

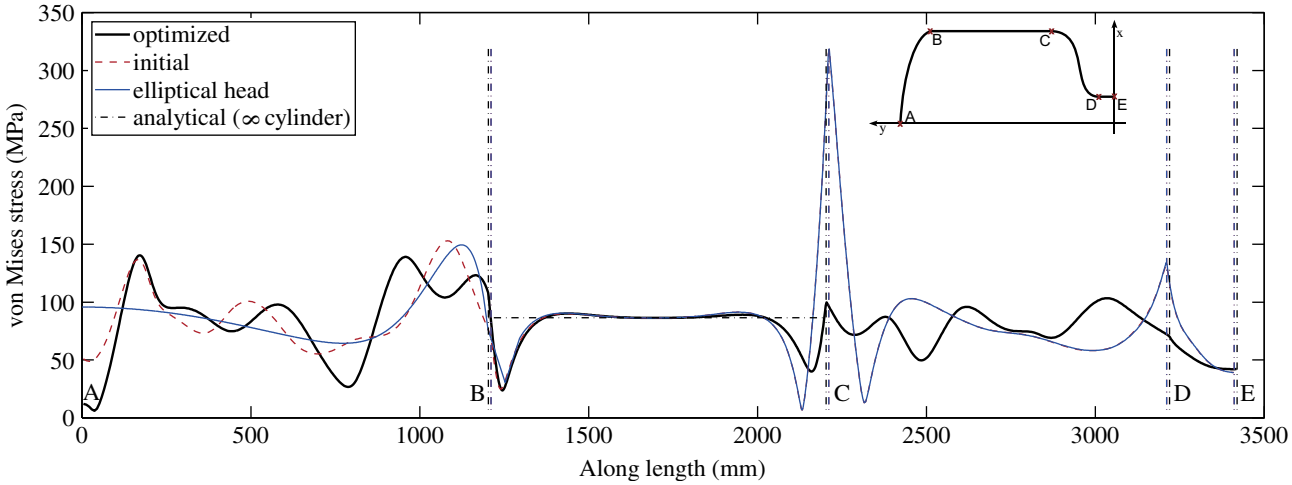

Fig. 17. von-Mises stress values along vessel optimized meridional profile obtained for example 2, considering $h_2 = 1000$ mm and null tangent angle at head symmetry point (no thermal load).

The tangent angle γ of the head spline at the vessel symmetry axis point (see Fig. 5) is kept null during the optimization. The internal and external temperatures, T_i and T_e, are equal to 250 °C and 25 °C, respectively. Three, four and six knot splines are considered to describe the head shapes, whereas the nozzle shapes are parameterized using a four knot spline in all examples. This parametrization choice is motivated by the convergence characteristics of the problem, which is easier for the nozzle shape than for the head one. The initial values of design variables are given in Table 2 considering three different initial shapes (close to a semi-sphere) corresponding to three, four and six head spline knots (design variables).

Initially, the convergence of the von-Mises stress values (maximum values among the three Gauss integration points through the thickness) along the vessel meridional profile is analyzed by considering different discretizations of the finite element mesh with and without thermal load. The results obtained for the von-Mises stresses are shown in Figs. 6 and 7 (the beginning of the plot is the center point of the head), disregarding and including the thermal load, respectively. In both analyses 4, 4, 4, and 2 divisions are adopted for head, cylindrical region h_2, nozzle, and h_4 region, respectively; and the discretizations employed are 10, 20, 50, and 100 finite elements for each division. By analyzing von-Mises stress values, it can be concluded that stress curves converged to the same values along vessel meridional profile. Numerical discretizations with 1100, 1150, and 1250 finite elements for the problems with three, four and six head spline knots (design variables) (corresponding to initial shapes 1, 2, and 3 – see Table 2) are adopted, respectively, with and without thermal load. These discretization choices are considered to provide accurate enough stress results throughout the optimization processes.

5.1.1. Entire vessel design without temperature gradient

First, a temperature gradient is not considered along the vessel thickness. The optimization results obtained are shown in Fig. 8 considering different number of head spline knots (corresponding to initial shapes 1, 2, and 3). Fig. 9(a, b and c) show the variation of von-Mises stresses along the meridional profile of the entire vessel for three, four, and six knot splines corresponding to initial shapes 1, 2, and 3, respectively.

The analytical stress $\sigma^a_{h_2}$ (along the cylindrical region h_2, see Fig. 5) of an infinite cylinder calculated using membrane theory is equal to 86.6 MPa [10]. For all plots in this work, "analytical" means the von-Mises stress result for an infinite cylinder. The maximum von-Mises stress in the head and nozzle are presented in Table 4. Fig. 10 shows the convergence of the multi-objective function for head spline with 3 knots (and initial shape 1). It illustrates the effect of the p-continuation strategy in the optimization process - see Eq. (1).

5.1.2. Entire vessel design considering temperature gradient

Now, a temperature gradient is added along the thickness of the vessel model. The objective is to analyze the effect of thermal loading in the final design vessel shape. The results obtained by shape optimization are illustrated in Fig. 11 considering different numbers of head spline knots (corresponding to initial shapes 1, 2, and 3). Fig. 12(a, b, and c) show the variation of von-Mises stresses along the meridional profile of the entire vessel for different numbers of head spline knots (and initial shapes). Fig. 13 shows the convergence of the multi-objective function considering a number of head spline knots equal to 6 (and initial shape 3).

5.1.3. Discussion

The maximum von-Mises stress values in the head and nozzle are presented in Table 4, and are indicated in the plots of Figs. 9 and 12. As expected, in all cases the obtained optimized stress distributions are usually not better than a semi-spherical head (which, however, is difficult to manufacture). From Fig. 9, it is noticed that for the three cases analyzed without thermal load, the maximum head stresses are smaller than the cylinder stresses. As the number of spline knots increases, the stress value oscillation also increases, an effect that is not observed in the design problem with the thermal gradient, as shown in Fig. 12. In addition, the stress values in the junction between head and cylinder decrease (see Table 4) and the convergence stability is improved either in the presence or absence of the thermal gradient.

Furthermore, a smooth stress distribution is obtained for the head using a small number of spline knots (3 and 4) either with or without thermal load, as shown in Figs. 9 and 11(a, b), Fig. 12(a and b). A similar conclusion was obtained by Zhu and Boyle [4] considering the separate head design without thermal load. When a six knot spline (corresponding to initial shape 3) and thermal load are considered, the maximum head stress (256.6 MPa) is smaller than even the semi-sphere stress (261.6 MPa) - see Table 4.

Concerning the nozzle, when the thermal gradient is not considered, its shape and stress distribution oscillates between two results which are shown by solid lines (optimized) in Fig. 9(a and b) This does not occur when the thermal gradient is considered, that is, only one local optimum is obtained, as shown in Fig. 12. Meanwhile, it is noticed that an increase in the number of spline knots in the nozzle may generate geometries with slightly higher stress values (see Table 4). In addition, when the thermal load is considered, the nozzle stresses for optimized shape approach the cylinder stresses.

Table 5
Maximum von-Mises stress values (MPa), where subscripts $_h$, $_n$, $_0$, $_{se}$, and h_2 indicate head, nozzle, initial shape, standard ellipse, and cylindrical region h_2, respectively ($\sigma^a_{h_2}$ = 86.6 Mpa for infinite cylinder).

Example	σ_h	σ_{h0}	σ_{se}	σ_n	σ_{n0}	σ_{h2}	σ_{h2_0}	h_2	γ
Fig. 16	143.2	153.4	150.6	141.3	319.0	90.4	91.3	1000	free
Fig. 17	140.4	153.0	150.6	103.4	319.0	90.2	91.3	1000	null
Fig. 19	242.0	252.0	213.6	201.0	392.8	200.0	201.0	1000	null
Fig. 22	141.2	161.1	150.1	109.5	336.0	92.5	95.0	500	null
Fig. 23	135.0	162.5	150.3	106.1	333.7	75.7	82.4	250	null
Figs. 16, 17 and 22 and 23	no thermal load								
Fig. 19	thermal load								

5.2. Example 2: pressure vessel considering influence of angle γ at the head top

In this example, an initial shape close (due to spline approximation) to an elliptical head shape ($h_1 = d_0/4$) is considered. A control of the γ tangent angle at the point of symmetry of the

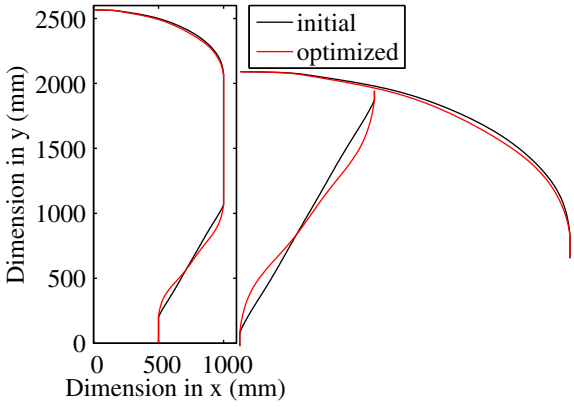

Fig. 18. Optimization result for example 2, considering h_2 = 1000 mm and thermal load with null tangent angle at head symmetry point (with thermal load). Detailed views of head and nozzle are given beside figure.

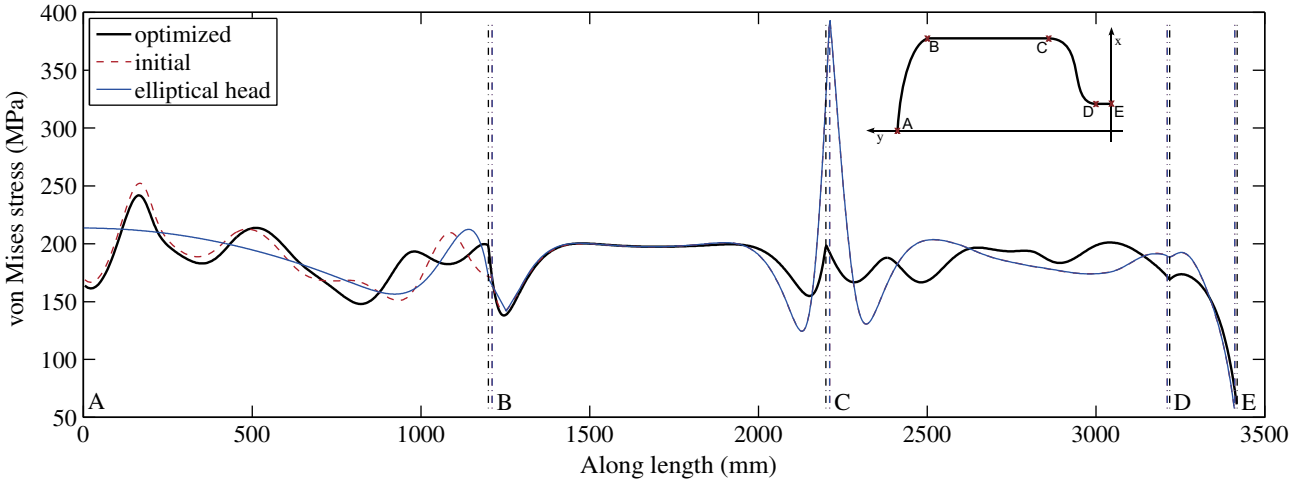

Fig. 19. von-Mises stress values along vessel optimized meridional profile obtained for example 2, considering $h_2 = 1000$ mm and null tangent angle at head symmetry point (with thermal load).

vessel (see Fig. 5) is implemented. Another important aspect in this example is to verify how the shape optimization result is affected by the variation of the dimension h_2 (see Fig. 5). Thus, for example, for large h_2 dimension (approaching an infinite cylinder), the problem may be uncoupled, and the optimization problem may be solved for the nozzle and the head separately. The thermal load is considered along the vessel thickness for one of the cases analyzed in this example.

Seven and four knot splines are considered to describe the head and nozzle shapes, respectively, giving a total of eleven design variables in the design optimization problem. The initial values of design variables corresponding to a shape close to an elliptical head shape are given in Table 2. A discretization equal to 1300 finite elements is adopted for all cases in this example, i.e. with and without thermal load.

5.2.1. Entire vessel design considering pressure and temperature loading

In this first case, a temperature gradient is not considered along the vessel thickness. Thus, the objective of this first case is to analyze the influence of the γ tangent angle at the head top (vessel symmetry axis point - see Fig. 5). The angle value will be considered either null or variable and h_2 is kept constant and equal to 1000 mm. Figs. 14–17 show the final results of the shape optimization and the von-Mises stress distribution, considering free and null angle. The results obtained by the optimization are compared through von-Mises stress plots with the corresponding standard elliptical head shape vessel which is known to provide an optimum stress distribution [4].

Therefore, from Figs. 16 and 17 the maximum von-Mises stress values for optimized head shape considering initial shape with free angl (143.2 MPa), with null angl (140.4 MPa), and corresponding standard elliptical head shape (150.6 MPa) are, respectively, 65.4%, 62.1%, and 73.9%, greater than the corresponding analytical stress $\sigma^a_{h_2}$ of the infinite cylindrical vessel. The difference between the analytical (86.6 MPa) and numerical stress for the cylindrical region ($h_2 = 1000$ mm) (90.2 MPa), is 4%. For the nozzle, the optimized von-Mises stress is 63.2% and 19.4% greater than $\sigma^a_{h_2}$ considering free (variable) (141.3 MPa) and null angle (103.4 MPa), respectively, as detailed in Table 5. In both cases, optimal results obtained by shape optimization are better than using a corresponding elliptical head, and obtained stress values for the head and nozzle, considering null angle, are lower than maximum stress value for a vessel with corresponding elliptical head. The stress values obtained with null angle condition are lower than stress values obtained considering free (variable) angle. It seems that the null angle solution is a local minimum which is difficult to reach. The optimization taking the design variable γ into account must be conducted with care, thus, the null angle condition will be considered for the next results.

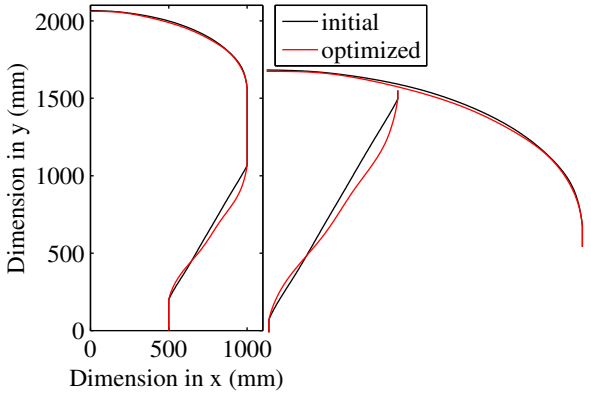

Fig. 20. Optimization result for example 2, considering $h_2 = 500$ mm (no thermal load). Detailed views of head and nozzle are given beside figure.

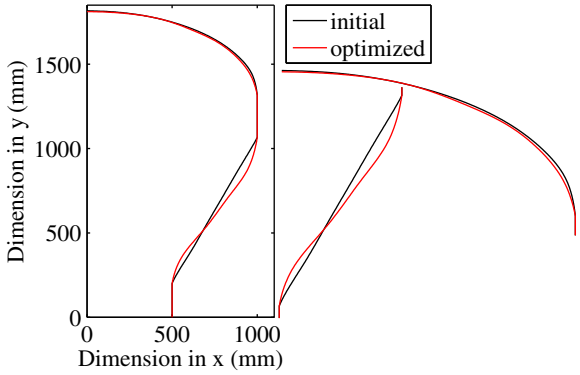

Fig. 21. Optimization result for example 2, considering $h_2 = 250$ mm (no thermal load). Detailed views of head and nozzle are given beside figure.

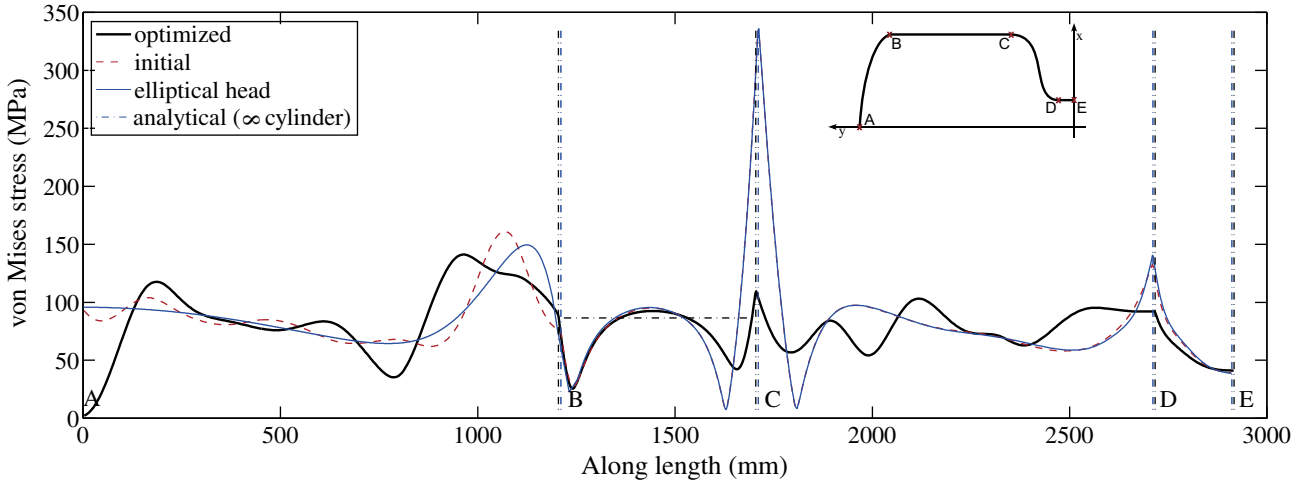

Fig. 22. von-Mises stress values along vessel optimized meridional profile obtained for example 2, considering $h_2 = 500$ mm (no thermal load).

Now, the entire vessel is designed considering the influence of thermal load. The internal and external temperatures, T_i and T_e, are equal to 200 °C and 25 °C, respectively. Figs. 18 and 19 show the optimized shape and von-Mises stresses along the meridional profile of entire vessel, respectively, considering null angle condition. It is noticed that at the head, the maximum stress for optimized shape (242 MPa) is larger than the maximum stress for elliptical head shape (213.6 MPa). In addition, the maximum stress at nozzle (201 MPa) is close to σ_{h_2} stress along the h_2 dimension (200 MPa), as detailed in Table 5.

5.2.2. Entire vessel design considering the influence of segment h_2

In this case the tangent angle of the vessel symmetry point is kept null ($\gamma = 0$), and the dimension h_2 is analyzed considering dimensions equal to 500 and 250 mm Figs. 20–23 show the final results of the shape optimization and the von-Mises stress distribution for the present study.

By comparing the von-Mises stress results for the head, we conclude that maximum head von-Mises stress values of the optimized result (141.2 MPa and 135 MPa) is 63.1% and 55.9% greater than $\sigma^a_{h_2}$ (infinite cylinder) for h_2 equal to 500 and 250 mm, respectively. In both cases the corresponding maximum elliptical head stress (150.1 MPa and 150.3 MPa) is 73.3% and 73.6% greater than $\sigma^a_{h_2}$ (infinite cylinder), respectively, thus the obtained stress values for the head shape are lower than the stress values for elliptical shape. For the nozzle, the optimized result (109.5 MPa and 106.1 MPa) is 26.4% and 22.5% greater than $\sigma^a_{h_2}$ (infinite cylinder) for h_2 equal to 500 and 250 mm, respectively, as detailed on Table 5. Thus, head and nozzle stresses are not significantly changed due to h_2 change. However, again, optimal result head stresses obtained by shape optimization are better (lower maximum stress value) than using a corresponding standard elliptical head vessel.

The cylinder stresses are sensitive to the h_2 value. It is important to observe that stress values for optimal results in the central region for h_2 equal to 1000, 500, and 250 mm are different, being equal to 90.2, 92.5, and 75.7 MPa, respectively, and thus, 4.2% and 6.8% larger than, and 12.6% smaller than $\sigma^a_{h_2}$ (infinite cylinder), respectively. By increasing h_2 values we observe the widening of a region with constant stresses, as expected (see Figs. 17, 22 and 23) with the stress value reaching the stress value of the "infinite cylinder".

Thus, it should be remarked that for the h_2 dimensions analyzed (250 mm and 500 mm) it is important to consider the shape optimization of the entire vessel, allowing the optimization method to minimize the different stress levels between head and nozzle by considering the coupling region (h_2).

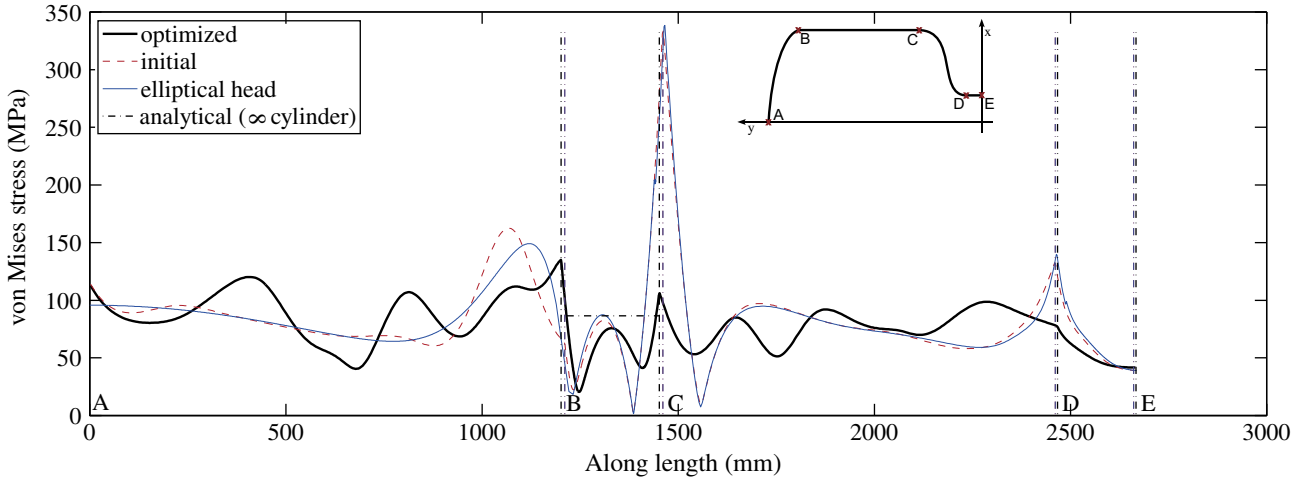

Fig. 23. von-Mises stress values along vessel optimized meridional profile obtained for example 2, considering $h_2 = 250$ mm (no thermal load).

6. Conclusions

In this work, an integrated shape optimization study of pressure vessels is conducted considering a model of the entire pressure vessel. A proper multi-objective function based on a logarithmic of a p-root of summation of p-exponent terms has been defined for minimizing the tank maximum von-Mises stress.

For vessels with mechanical loading only and initial shapes close to a semi-sphere, one notices that the maximum head stresses are smaller than the cylinder stresses. In addition, as the number of spline knots increases, the stress value oscillation also increases, a pattern which is not observed in the design problems with thermal gradient included. However, as the number of spline knots increases, the stress values in the junction between head and cylinder decrease and the convergence stability is improved either with or without a thermal gradient. Remarkably, a smooth stress distribution is obtained for the head region even when using just a small number of spline knots (3 and 4). Another interesting aspect observed for the cases investigated is that the nozzle stresses approach the cylinder stresses when the thermal load is considered.

By comparing the standard elliptical head results, we concluded that the stress values are smaller for the optimized result than for the elliptical head when no thermal load is considered. In addition, lower stress values are obtained considering the null angle condition ($\gamma = 0$). Thus, the null angle condition seems to give a better vessel design for stress value criteria.

When analyzing the influence of segment h_2 in the absence of thermal gradients, one notices that the cylinder stresses are more sensitive to the h_2 value than head and nozzle stresses. *Thus, depending on the value of the connecting segment h_2, it is important to consider the shape optimization of the entire vessel, allowing the optimization method to minimize the different stress levels between head and nozzle by considering the coupling cylindrical region (h_2), as successfully achieved in this work*.

As future work, the design of pressure vessels taking into account non-linear effects, such as pressure limit, will be performed. These issues are presently under consideration.

Acknowledgment

All authors thank PETROBRAS for supporting this research through GALILEU project n. 0050.0042368.08.4. The first author also acknowledges FUSP (Foundation of University of São Paulo). In addition, the last author thanks CNPq (project number no 303689/2009-9).

References

[1] Middleton J, Owen DRJ. Automated design optimization to minimize shearing stress in axisymmetric pressure-vessels. Nuclear Engineering and Design 1977;44(3):357–66.
[2] Middleton J. Optimal-design of torispherical pressure-vessel end closures. Engineering Optimization 1979;4(3):129–38.
[3] Blachut J. Minimum weight of internally pressurised domes subject to plastic load failure. Thin-walled Structures 1997;27(2):127–46.
[4] Zhu L, Boyle JT. Optimal shapes for axisymmetric pressure vessels: a brief overview. Journal of Pressure Vessel Technology-transactions of the Asme 2000;122(4):443–9.
[5] Mackenzie D, Boyle JT. A method of estimating limit loads by iterative elastic analysis .1. Simple examples. International Journal of Pressure Vessels and Piping 1993;53(1):77–95.
[6] Nadarajah C, Mackenzie D, Boyle JT. A method of estimating limit loads by iterative elastic analysis .2. Nozzle sphere intersections with internal-pressure and radial load. International Journal of Pressure Vessels and Piping 1993;53(1):97–119.
[7] Shi JH, Mackenzie D, Boyle JT. A method of estimating limit loads by iterative elastic analysis .3. Torispherical heads under internal-pressure. International Journal of Pressure Vessels and Piping 1993;53(1):121–42.
[8] Malinowski M, Magnucki K. Optimal design of sandwich ribbed flat baffle plates of a circular cylindrical tank. International Journal of Pressure Vessels and Piping 2005;82(3):227–33.
[9] Banichuk NV, Ragnedda F, Serra M. Optimization of mass effectiveness of axisymmetric pressure vessels. Structural and Multidisciplinary Optimization 2008;35(5):453–9.
[10] Magnucki K, Lewinski J. Fully stressed head of a pressure vessel. Thin-walled Structures 2000;38(2):167–78.
[11] Magnucki K, Szyc W, Lewinski J. Minimization of stress concentration factor in cylindrical pressure vessels with ellipsoidal heads. International Journal of Pressure Vessels and Piping 2002;79(12):841–6.
[12] Hammer V, Olhoff N. Topology optimization of continuum structures subjected to pressure loading. Structural and Multidisciplinary Optimization 2000;19(2):85–92.
[13] Du J, Olhoff N. Topological optimization of continuum structures with design-dependent surface loading - part II: algorithm and examples for 3D problems. Structural and Multidisciplinary Optimization 2004;27(3):166–77.
[14] Zheng B, Chang CJ, Gea HC. Topology optimization with design-dependent pressure loading. Structural and Multidisciplinary Optimization 2009;38(6):535–43.
[15] Duysinx P, Bendsoe MP. Topology optimization of continuum structures with local stress constraints. International Journal for Numerical Methods in Engineering 1998;43(8):1453–78.
[16] Stump FV, Silva ECN, Paulino GH. Optimization of material distribution in functionally graded structures with stress constraints. Communications in Numerical Methods in Engineering 2007;23(6):535–51. doi:10.1002/cnm.910.
[17] Amstutz S, Novotny AA. Topological optimization of structures subject to Von Mises stress constraints. Structural and Multidisciplinary Optimization 2010;41(3):407–20. doi:10.1007/s00158-009-0425-x.
[18] Blachut J, Magnucki K. Strength, stability, and optimization of pressure vessels: review of selected problems. Applied Mechanics Reviews 2008;61(6):060801.
[19] Soric J. Stability analysis of a torispherical shell subjected to internal-pressure. Computers & Structures 1990;36(1):147–56.
[20] Spence J, Tooth A. Pressure vessel design: concepts and principles. Elsevier Applied Science; 1993.
[21] MATLAB. R2010a documentation. The MathWorks, Inc.; 2010.
[22] Ansys. ANSYS advanced analysis techniques guide. ANSYS, Inc.; 2005.
[23] Haftka RT, Gürdal Z. Elements of Structural optimization. 3rd ed. Kluwer Publishers; 1992.